Eur Radiol (2005) 15: 1815–1825
DOI 10.1007/s00330-005-2666-4

J. Randy Jinkins
Jay S. Dworkin
Raymond V. Damadian

Upright, weight-bearing, dynamic–kinetic MRI of the spine: initial results

Received: 8 September 2004
Revised: 31 December 2004
Accepted: 31 December 2004
Published online: 20 May 2005

J. R. Jinkins
Department of Radiology,
Downstate Medical Center,
State University of New York,
450 Clarkson Avenue,
Brooklyn, NY 11203, USA

J. R. Jinkins (✉) · J. S. Dworkin ·
R. V. Damadian
Fonar Corporation,
110 Marcus Drive,
Melville, NY 11747, USA
e-mail: jrjinkins@aol.com
Tel.: +1-631-6942929
Fax: +1-631-3907766

Abstract The potential relative beneficial aspects of upright, weight-bearing (pMRI), dynamic–kinetic (kMRI) spinal imaging over that of recumbent MRI (rMRI) include the revelation of occult spinal disease dependent on true axial loading, the unmasking of kinetic-dependent spinal disease and the ability to scan the patient in the position of clinically relevant signs and symptoms. This imaging unit under study also demonstrated low claustrophobic potential and yielded comparatively high resolution images with little motion/magnetic susceptibility/chemical shift artifact. Overall, it was found that rMRI underestimated the *presence* and *maximum degree* of gravity-dependent spinal pathology and missed altogether pathology of a *dynamic* nature, factors that are optimally revealed with p/kMRI. Furthermore, p/kMRI enabled optimal linkage of the patient's clinical syndrome with the medical imaging abnormality responsible for the clinical presentation, thereby allowing for the first time an improvement at once in both imaging *sensitivity* and *specificity*.

Keywords Magnetic resonance imaging · Spine · Degenerative disease · Kinetic imaging · Weight-bearing imaging · Positional imaging

Introduction

Until the present time period, MRI using available commercial systems has been limited to acquiring scans with patients in the recumbent position. Obviously, the human condition is continuously subject to the effects of gravity in positions other than that of recumbent. It is also clear that patients experience signs and symptoms during dynamic physiologic maneuvers of the body, conditions that are not possible to assess if patients are only imaged in a position of recumbency. In order to address this situation, a new fully open MRI unit was developed to allow upright as well as recumbent imaging. This configuration at the same time enables partial or full weight bearing and simultaneous kinetic maneuvers of the patient's whole body or any individual body part. The objective of this technological advance was to facilitate imaging of the body in any position of normal stress, across the limits of range of motion, and importantly in the specific position of the patient's clinical syndrome. It was anticipated that, to some degree, radiologically occult but clinically relevant weight-bearing and/or kinetically dependent disease not visible on the recumbent examination would be unmasked by the positional–kinetic imaging technique. Furthermore, it was hoped that under optimized conditions a specific imaging abnormality present only on the axial loaded, kinetic imaging study might thereby be more clearly linked with specific clinical signs and symptoms for which the patient is undergoing the imaging examination [1, 2].

The Upright MRI system

All examinations were performed on a recently introduced full-body MRI system (Upright MRI, Fonar Corporation, Melville, NY, USA). The system operates at 0.6-T field strength using an electromagnet with a horizontal field, transverse to the longitudinal axis of the patient's body.

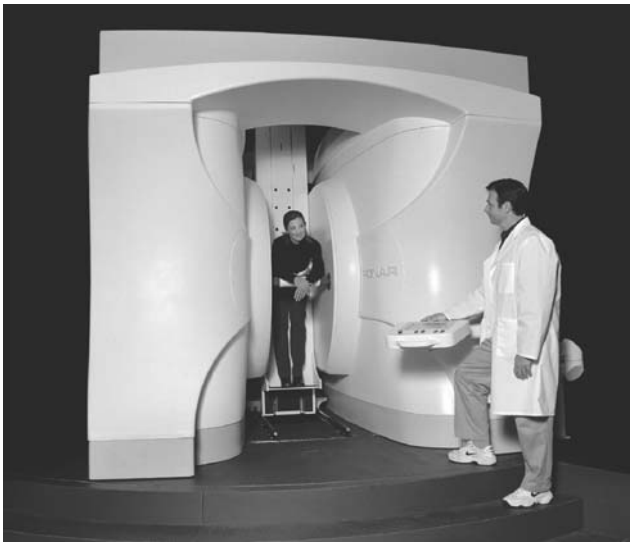

Fig. 1 Overview image of the Upright MRI unit

Depending upon the spinal level of clinical interest, all examinations were performed using either a cervical or lumbar, planar or solenoidal radiofrequency receiver coil. The MRI unit was configured with a top-front open design that incorporated a patient-scanning table which enabled tilt, translation and elevation functions with the patient mounted on the table. This unique patient handling system allowed vertical (i.e., upright, weight-bearing), horizontal (i.e., recumbent) and angled (i.e., −20 to 90°) patient positioning for scanning. Dynamic–kinetic flexion and extension maneuvers of the spine were also possible with the top-front open construction design (Fig. 1). Thus, traditional recumbent neutral MRI (rMRI) could be supplemented utilizing the Upright MRI system with physiologic upright-neutral positional MRI (pMRI) and dynamic–kinetic MRI (kMRI) (Table 1). This discussion will outline some of the key issues discovered using p/kMRI of the spine, and point out how the findings differ from that of rMRI.

Applications

Simply from a clinical standpoint, rMRI is theoretically inadequate for a complete and thorough evaluation of the spinal column and its contents. Biomechanically, the human condition is continuously subject to both weight bearing and variations in body positioning, or pMRI, as well as complex kinetic maneuvers, or kMRI, in three dimensions [3–6]. The Stand-Up MRI unit was intended to address these important clinical considerations. In practice, occult weight-bearing disease (e.g., focal intervertebral disc herniations, spinal stenosis, thecal sac volumetric change), as well as dynamic–kinetic dependent disease (e.g., disc herniations, spinal stenosis, hypermobile intersegmental

Table 1 Patient-positioning-related variations of MRI

Recumbent MRI	Supine, recumbent imaging
Positional MRI	Imaging in varying angular positions of the longitudinal axis of the body
Kinetic MRI	Imaging during dynamic–kinetic somatic maneuvers (e.g., flexion, extension, rotation, lateral bending)

spinal instability) of a degenerative nature [7–23] were unmasked by the p/kMRI technique. In addition, a true assessment of the patient's *weight-bearing, postural spinal curvature* was possible on upright-neutral pMRI, thereby enabling better evaluation of whether the loss of curvature was due to patient positioning (i.e., rMRI) or as a probable result of somatic perispinal muscular guarding or spasm (Figs. 2, 3). Prior studies by other researchers using axial loading and dynamic flexion–extension kinetic maneuvers have borne out the very real significance of these varied observations [24–38].

To begin with, upright-neutral pMRI revealed a phenomenon here termed *spinal column telescoping*, whereby a collapse of the spine into itself was observed at levels of generalized *intervertebral disc degeneration* (i.e., both disc desiccation and disc space narrowing) (Fig. 4) [39]. This telescoping effect was observed to be consonant with the overall additive amount of loss of disc space height present among the levels of disc degeneration. In addition, as a direct consequence of this *physiologic* axial loading (i.e., the additive effects of simple upper body weight plus the effective axial weight of balancing muscular tension upon the spinal column when upright), increasing redundancy of the discal, ligamentous and meningeal tissues of the spine resulted in increased degrees of central canal and lateral recess (i.e., subarticular zone) spinal stenosis; at the same time, superior–inferior (i.e., craniocaudal) shortening of the spine associated with degenerative telescoping caused increased degrees of neural foramen stenosis at levels of disc degeneration (Fig. 3). On occasion, the size of a posterior *disc protrusion–herniation* was seen to enlarge on upright-neutral pMRI (Fig. 3) compared with the recumbent scan in the same patient. This is in part explained by the laws of fluid dynamics that simplistically state that fluids are not compressible; when the disc space volume is reduced at levels of degeneration during axial loading, relative to the recumbent imaging examination, the semifluid disc material under compression must by definition *exit* the narrowed disc space. This phenomenon was also observed in cases of de novo disc herniation where posterior disc herniations were only observed on upright imaging studies (Fig. 5). These findings would seem to be an important observation, obviously improving the qualitative and quantitative nature of the analysis in clinically relevant cases of disc herniation. Finally, relative to rMRI in the same patients, upright-neutral pMRI frequently revealed the presence of sagittal plane *hypermobile spondy-*

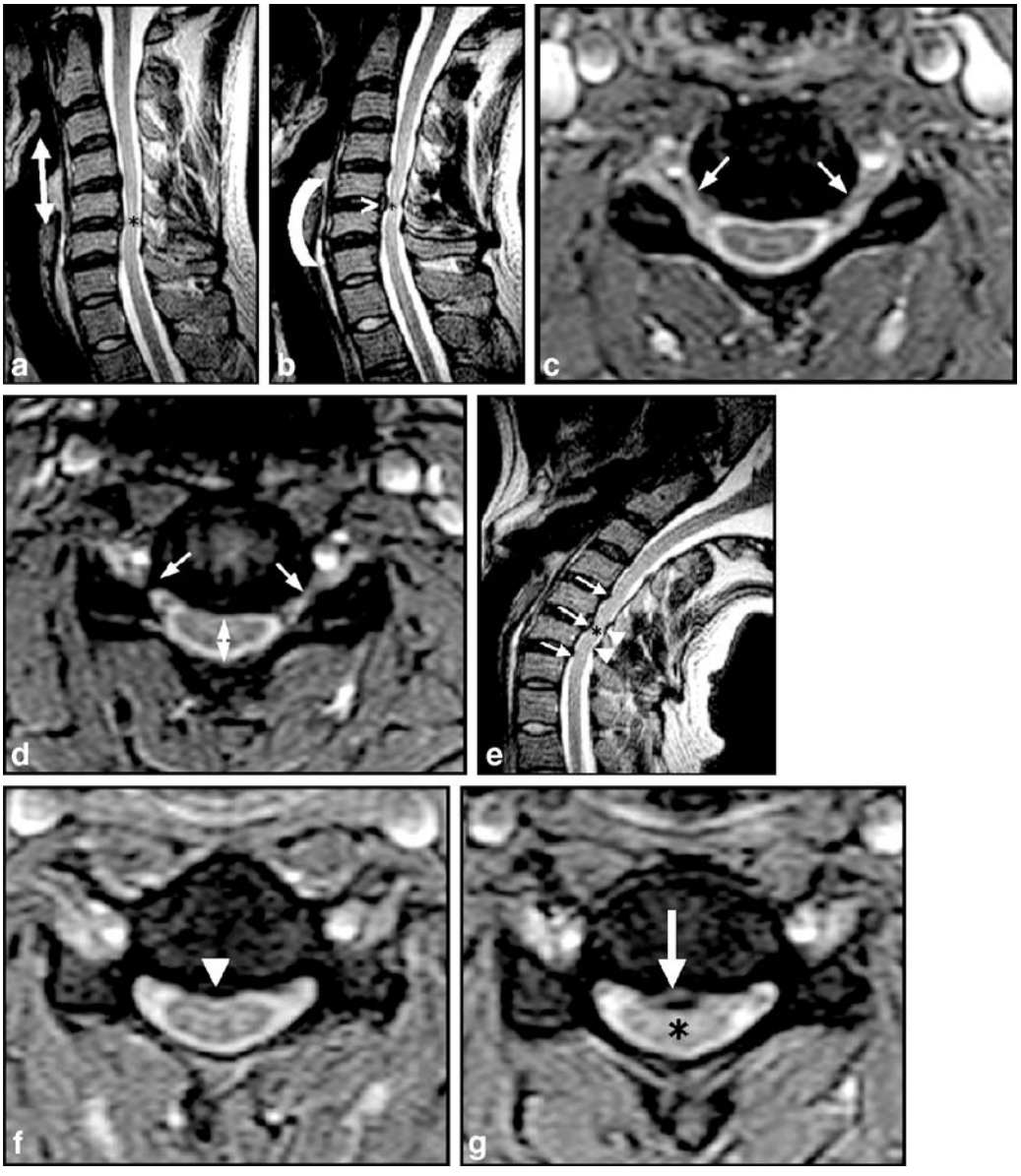

Fig. 2 Upright sagittal cervical spinal curvature analysis; unmasking of central spinal stenosis; *occult herniated intervertebral disc* (all images of the same patient). **a** Recumbent midline sagittal T2-weighted fast spin echo MRI (*rMRI*) shows straightening and partial reversal of the sagittal spinal curvature of the cervical spine (*double-headed arrow*). Minor posterior disc bulges/protrusions are present at multiple levels, but the spinal cord (*asterisk*) is not compressed. **b** Upright-neutral midline sagittal T2-weighted fast spin echo MRI (*pMRI*) shows partial restoration of the true sagittal postural cervical curvature upon neutral-upright positioning (*curved line*). Note the relative increase in the posterior disc protrusion at the C5–C6 level (*arrowhead*) and encroachment on the spinal cord (*asterisk*) compared with the case on the recumbent image (**a**). **c** Recumbent axial T2*-weighted gradient recalled echo MRI (*rMRI*) through the C4–C5 level shows patent neural foramina bilaterally (*single-headed arrows*), and mild stenosis of the central spinal canal (*double-headed arrow*). **d** Upright-neutral axial T2*-weighted gradient recalled echo MRI (pMRI) through the C4–C5 level shows bilateral narrowing of the neural foramina (*single-headed arrows*). Note also the narrowing of the central spinal canal (*double-headed arrows*) relative to the recumbent study (**c**), and the compression of the underlying spinal cord (i.e., relative anteroposterior flattening of the spinal cord compared with the case on the recumbent image; **c**). **e** Upright-extension midline sagittal T2-weighted fast spin echo MRI (*kMRI*) shows further posterior protrusion of the intervertebral discs at multiple levels (*arrows*) and anterior infolding of the posterior spinal ligaments (*arrowheads*), resulting in overall worsening of the stenosis of the central spinal canal. Note the impingement (i.e., compression) of the underlying spinal cord (*asterisk*) by these encroaching spinal soft tissue elements. **f** Recumbent axial T2*-weighted gradient recalled echo MRI (rMRI) at the C5–C6 disc level shows posterior paradiscal osteophyte formation (*arrowhead*) extending into the anterior aspect of the central spinal canal. Note that the cervical spinal cord is atrophic, but there is a rim of CSF hyperintensity entirely surrounding the cord. **g** Upright-extension axial T2*-weighted gradient recalled echo MRI (kMRI) revealing (extension-related) focal posterior disc herniation (*arrow*). Note the overall increased stenosis of the central spinal canal and the compression indentation of the underlying cervical spinal cord (*asterisk*).

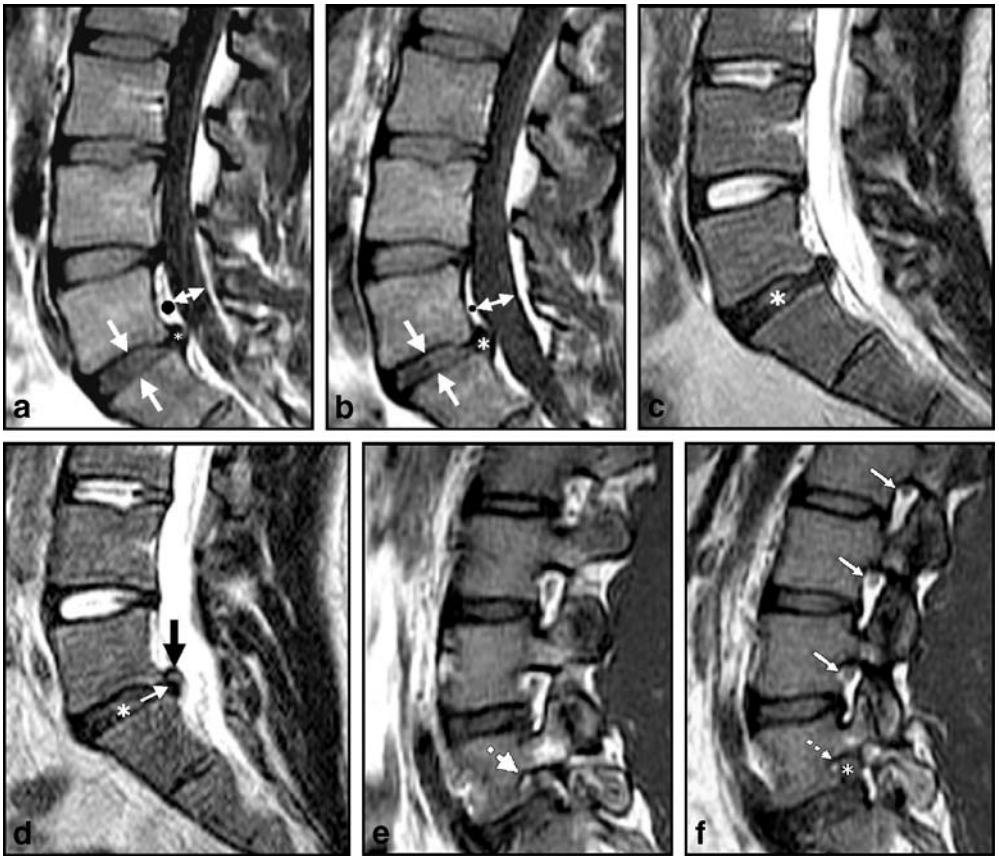

Fig. 3 Effects of gravity on the intervertebral disc, thecal sac, and spinal neural foramina; true *sagittal postural lumbosacral curvature*. **a** Recumbent midline sagittal T1-weighted fast spin echo MRI (rMRI) shows a focal disc herniation at L5–S1 (*asterisk*) and mild narrowing of the superoinferior disc height at this level (*single-headed arrows*). Note also the anteroposterior dimension of the thecal sac (*double-headed arrow*), and the size of the anterior epidural space (*dot*) at the L4 level. **b** Upright-neutral (standing) midline sagittal T1-weighted fast spin echo MRI (pMRI) shows minor further narrowing of the height of the L5–S1 intervertebral disc (*single-headed arrows*) and enlargement of the posterior protrusion of the disc herniation at this level (*asterisk*) (compare with **a**). Also note the generalized expansion of the thecal sac (*double-headed arrow*) because of gravity-related hydrostatic CSF pressure increases, and the consonant decrease in the dimensions of the anterior epidural space (*dot*; theoretically caused by a reduction in volume of the anterior epidural venous plexus). Finally, note that the upright-standing spine now assumes the true sagittal postural curvature on this image, compared with the case on the recumbent image (compare with **a**). **c** Recumbent midline sagittal T2-weighted fast spin echo MRI (rMRI) shows the posterior disc herniation at L5–S1 (*asterisk*). **d** Upright-neutral midline sagittal T2-weighted fast spin echo MRI (*pMRI*) shows further narrowing of the L5–S1 intervertebral disc (*asterisk*; compare with **c**) and a new component to the posterior disc herniation (*black arrow*) resulting in overall enlargement of the size of the herniation (compare with **c**). Apparently, this observed enlargement is caused by intradiscal fluid (i.e., water) and/or disc material exiting via an unvisualized posterior radial annular tear (*white arrow*) into the epidural space. Because fluids and semifluids (water; nucleus pulposis) are noncompressible, the reduction in the size of the disc volume makes it necessary that the intradiscal fluids–semifluids evacuate via some route, a radial annular tear being the most likely pathway. Some degree of radial peripheral disc bulging may also contribute to this phenomenon. **e** Recumbent midline parasagittal T1-weighted fast spin echo MRI (rMRI) on the patient's left side shows narrowing of the L5–S1 spinal neural foramen (*dashed arrow*) as a result of posterior disc protrusion, intervertebral disc space narrowing and paradiscal osteophyte formation. **f** Upright-neutral midline parasagittal T1-weighted fast spin echo MRI (pMRI) on the patient's left side reveals minor generalized narrowing of all of the spinal neural foramina (*solid arrows*), including the L5–S1 level (*dashed arrow*) (compare with recumbent examination, **e**). At some point in this stenotic process, the exiting neurovascular bundle (*asterisk*) will undergo compression and may become symptomatic.

lolisthesis (see below), both in cases of degenerative spondylolisthesis as well as in cases of spondylolytic spondylolisthesis (Fig. 6) [40].

In a similar manner to that just noted, at some levels of intervertebral disc degeneration upright-neutral and upright-extension p/kMRI showed greater relative degrees of central spinal canal and neural foramen stenosis, while upright-flexion kMRI in some instances revealed a lessening or complete resolution of the same central canal and spinal neural foramen narrowing (Figs. 3, 7) [41, 42]. In exceptional cases, de novo posterior *disc herniations* were revealed only on upright-extension kMRI (Fig. 2). When present in the cervical spine, such cases of posterior disc herniation almost invariably showed some degree of com-

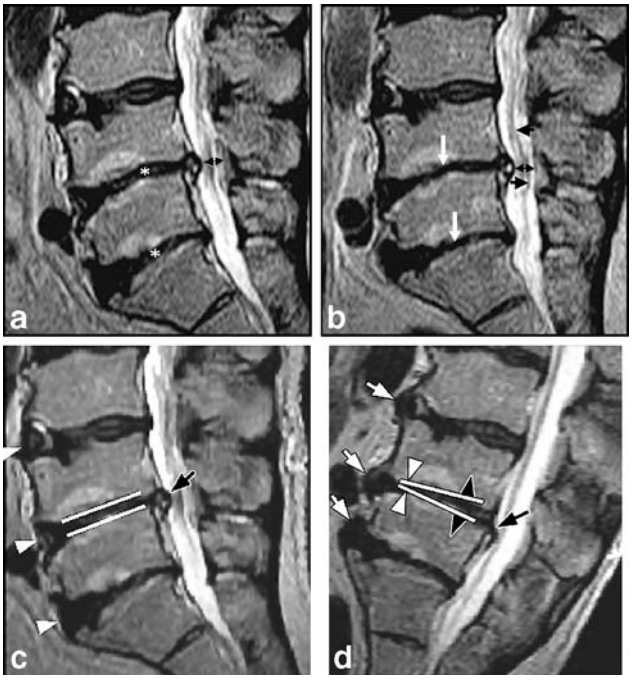

Fig. 4 Telescoping of the spinal column; reducing posterior disc herniation; increasing anterior disc protrusions; *dysfunctional intersegmental motion*. **a** Recumbent midline sagittal T2-weighted fast spin echo MRI (rMRI) showing degenerative disc disease at all levels, especially severe at L4–L5 and the L5–S1 levels (*asterisks*). A focal posterior disc herniation is noted at the L4–L5 level. Note the narrowed (i.e., stenotic) anteroposterior dimension of the thecal sac at the L4–L5 level (*double-headed arrow*). Also note the diffuse hyperintensity of the interspinous spaces indicating rupture of the interspinous ligaments at multiple levels. **b** Upright-neutral midline sagittal T2-weighted fast spin echo MRI (pMRI) revealing further gravity-related narrowing of the intervertebral discs at multiple levels (*white arrows*), compared with the recumbent examination (rMRI; **a**). This represents *telescoping* of the spinal column. Note also the minor increase in narrowing of the anteroposterior dimension of the thecal sac (*double-headed arrow*), and the increased redundancy of the nerve roots of the cauda equina (*black arrows*). **c** Recumbent midline sagittal T2-weighted fast spin echo MRI (rMRI) showing the relative parallel surfaces of the vertebral end plates at L4–L5 (*white lines*), and the flat surfaces of the anterior aspects of the intervertebral discs at multiple levels (*arrowheads*). Note again the posterior disc herniation at the L4–L5 level (*arrow*). **d** Upright-flexion midline T2-weighted fast spin echo MRI (kMRI) showing increases in the size of the anterior disc protrusions at multiple levels (*white solid arrows*) and a reduction of the posterior disc herniation at the L4–L5 level (*black arrow*), compared with the r/pMRI studies. Also note the opening up (i.e., enlargement) of the posterior aspect (*black arrowheads*) and the closing (i.e., narrowing) of the anterior aspect of the L4–L5 disc space (*white arrowheads*), with resulting anterior angulation of the vertebral end plates (*white lines*). The latter phenomenon represents *dysfunctional intersegmental motion*. Finally, note the hypersplaying of the spinous processes [with consonant hyperexpansion of the interspinous space(s)], indicating stretching/partial rupture of the interspinous ligament(s).

pression of the underlying spinal cord. Overall, this observation was felt to be one of the most important of the many noted in this observational study. Perhaps not surprisingly, some of the posterior disc herniations became

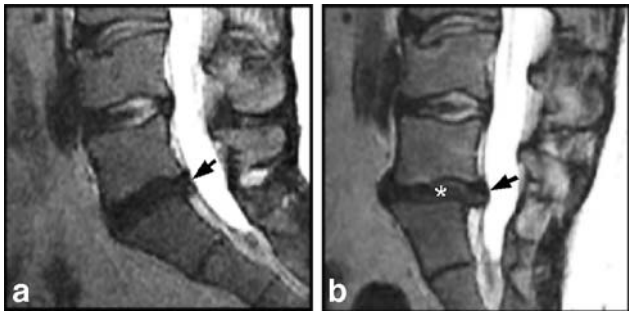

Fig. 5 Unoperated *positional intervertebral disc herniation*. **a** Recumbent midline sagittal T2-weighted fast spin echo MRI (rMRI) showing degenerative disc disease at the L5–S1 level associated with a minor posterior disc bulge/protrusion (*arrow*). **b** Upright-neutral midline sagittal T2-weighted fast spin echo MRI (pMRI) revealing gravity-related narrowing of the intervertebral disc space (*asterisk*) and a posterior disc herniation (*arrow*) not seen on the recumbent image. There may be a minor component of increased retrolisthesis relative to the recumbent study at this level as well.

Fig. 6 Unoperated translational *hypermobile spinal instability* associated with degenerative anterior spondylolisthesis related in part to theoretical ligamentous laxity (i.e., ligamentopathy). **a** Recumbent midline sagittal T1-weighted fast spin echo MRI (rMRI) shows minor intervertebral disc degeneration at the L4–L5 level (*asterisk*). **b** Upright-neutral midline sagittal T1-weighted fast spin echo MRI (pMRI) reveals anterior slip of L4 on L5 (*arrow*) compared with the recumbent examination. **c** Upright-flexion midline sagittal T1-weighted fast spin echo MRI (kMRI) demonstrates further anterior subluxation of L4 on L5 (*arrow*) compared with Fig. 8a and b. This demonstrates the dynamic *translational hypermobile instability* in part related to *ligamentopathy*, and in this case associated with *discopathy*, that may be entirely occult on recumbent imaging.

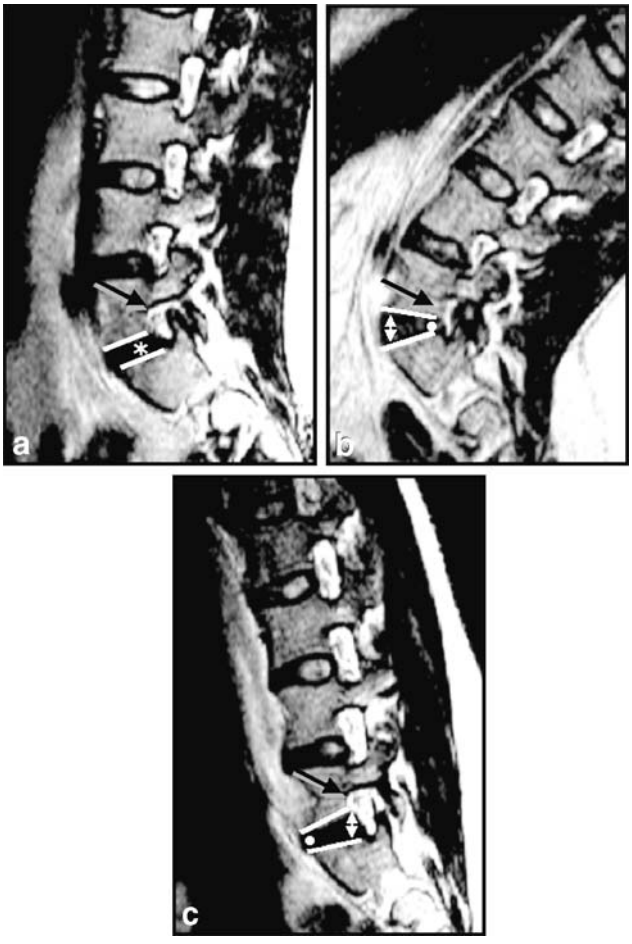

Fig. 7 Effects of dynamic–kinetic maneuvers (kMRI) on spinal neural foramina at levels of degenerated disc disease and theoretical ligamentous laxity (i.e., ligamentopathy); *dysfunctional intersegmental motion*. **a** Recumbent parasagittal T2-weighted fast spin echo MRI (rMRI) shows intervertebral disc degeneration at the L5–S1 level (*asterisk*). Note the mild narrowing of the neural foramen (*arrow*) at this level (i.e., minor foraminal stenosis), and the near parallel surfaces of the vertebral end plates (*lines*). **b** Upright-extension parasagittal T2-weighted fast spin echo MRI (kMRI) reveals further narrowing of the neural foramen at L5–S1 (*arrow*) relative to the recumbent image (Fig. 6a). Note the opening of the anterior aspect of the disc space (*double-headed arrow*), closing of the posterior aspect of the disc space (*dot*), and resulting posterior angulation of the vertebral endplates (*lines*). The neural foramina at other levels are minimally narrowed compared with the case on the recumbent image (Fig. 6a). **c** Upright-flexion parasagittal T2-weighted fast spin echo MRI (kMRI) demonstrates opening of the neural foramen at L5–S1 (*arrow*), the opening of the posterior aspect of the disc space (*double-headed arrow*), and closing of the anterior aspect of the disc space (*dot*). Note the anterior angulation of the vertebral end plates (*lines*). **b** illustrates *dysfunctional intersegmental motion* in addition to the dynamic changes in the size of the neural foramen at levels of disc degeneration and theoretical ligamentous laxity (i.e., ligamentopathy). The neural foramina at other levels are somewhat enlarged compared with the situation on the recumbent and the extension images (Fig. 6a, b)

consonantly less severe when upright-flexion kMRI was performed (Fig. 4) [43, 44]. This relative change will be worthy of preoperative note to those surgeons who operate on the spine in positions of partial flexion.

In some cases of intervertebral disc degeneration, another fluctuating alteration which was observed was that of sagittal plane *hypermobile intersegmental spinal instability* [45–55]. It proved in practice to be possible to judge even minor degrees of translational hypermobile spinal instability (e.g., mobile anterolisthesis or retrolisthesis) grossly as well as by using direct region-of-interest measurements (Fig. 7). The technique of kMRI obviously does not suffer from the artifact-inducing effects of imaging magnification and patient-positioning errors potentially inherent in conventional upright-dynamic, flexion–extension radiographic imaging studies traditionally used in these circumstances [56–63]. Progressive degenerative alterations in the intervertebral discs and posterior spinal facet joints will have either positive (i.e., hypermobile) or negative (i.e., hypomobile: *hypomobile intersegmental spinal stability*) effects upon intersegmental motion [64–67]. The latter may progress to *functional intersegmental spinal autofusion* whereby virtually all intersegmental spinal motion is lost at severely chronically degenerated spinal levels (Fig. 8).

Also noted at levels of intersegmental degeneration (i.e., combined degenerative alterations of the intervertebral disc, posterior spinal facet joints, spinal ligaments, intrinsic spinal muscles) was a sagittal plane hypermobile "rocking" of the adjacent vertebrae in relationship to each other on p/kMRI (Figs. 5, 10) [68]. Close observation of the opposed adjacent vertebral endplates in such cases showed them to move in relationship to each other to a much greater degree than is observed at levels with visibly normal interposed intervertebral discs as judged by MRI (Figs. 5, 10). This pathologic movement is here termed *dysfunctional intersegmental motion* (DIM). The significance of DIM is believed to be in the compelling theoretical possibility that such uncontrolled pathologic vertebral motion may engender generalized-progressive *accelerated intersegmental spinal degeneration* owing to the effects of excessive repetitive micro-autotrauma over long periods of time. The self-protecting/stabilizing spinal mechanisms inherent in the normal intervertebral discs, posterior spinal facet joints and intact spinal ligaments/muscles are partially lacking in such cases, perhaps initiating a progressive degenerative cascade of degenerative *autotramatizing intersegmental spinal hypermobility*.

The postoperative spine may perhaps be best analyzed by p/kMRI in those patients who have previously undergone instrumented and uninstrumented surgical intersegmental fusion procedures [69]. In the absence of ferromagnetic fusion implants, the Upright MRI unit was capable of acquiring a same-parameter postoperative p/kMRI study to compare with the preoperative p/kMRI examination. Cases of successful rigid intersegmental fusion, for example, showed no evidence of intersegmental motion, thereby

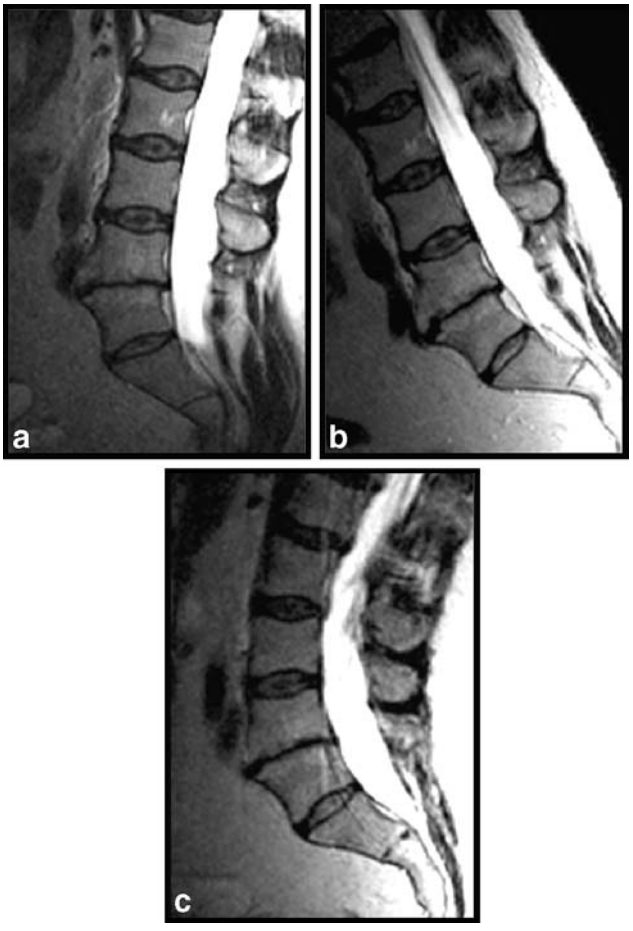

Fig. 8 Unoperated degenerative *hypomobile intersegmental spinal stability*. **a** Recumbent midline sagittal T2-weighted fast spin echo MRI (rMRI) shows marked degenerative intersegmental alterations at the L5–S1 level. **b** Upright-flexion midline sagittal T2-weighted fast spin echo MRI (kMRI) demonstrates intersegmental hypomobility at the L5–S1 level. **c** Upright-extension midline sagittal T2-weighted fast spin echo MRI (kMRI) again reveals no intersegmental motion at the L5–S1 level relative to the other spinal segments.

confirming postoperative intersegmental stability of the surgical construct. On the other hand, hypermobile intersegmental spinal instability *adjacent* to levels of a stable fusion was clearly revealed by the dynamic kMRI technique (Fig. 9). Another example of adjacent segment disease above or below levels of surgical fusion was recurrent disc herniation with compression of the underlying spinal cord, only observed on p–kMRI (Fig. 10).

Even discectomy alone, unaccompanied by surgical bony fusion, will over time predictably negatively impact the overall mobility and pathologic change of the spine; these complex physiologic spinal parameters are eminently well evaluated with the dynamic-weight-bearing MRI method [70]. For example, another finding in the postoperative spine included the revelation of recurrent disc herniation following prior partial discectomy *only* visualized with the patient in the upright position during pMRI (Fig. 11).

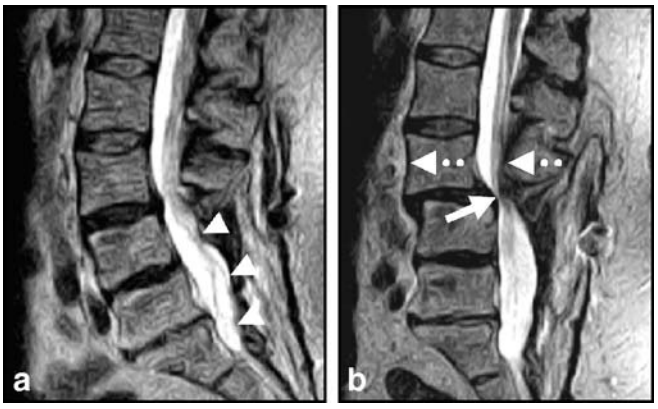

Fig. 9 Adjacent level *postoperative intersegmental hypermobile instability* at the segment above spinal fusion occurring 5 years following bilateral pedicle screw and rod placement extending between L4 and S1, and bilateral laminectomy at the L4–S1 levels. **a** Recumbent midline sagittal T2-weighted fast spin echo MRI (rMRI) shows bilateral laminectomy extending from L4 to S1 (*arrowheads*). The patient also had bilateral pedicle screws and rods extending from and to the same levels (not shown). No metallic artifact is present because the surgical materials were composed of titanium. **b** Sagittal-upright-sitting (i.e., partial flexion) midlineT2-weighted fast spin echo MRI (p/kMRI) demonstrates marked anterior slip of the L3 vertebral body upon the L4 vertebra (*dashed arrows*). Also note the resultant marked stenosis of the central spinal canal at the L3–L4 level (*solid arrow*), and resultant encroachment of the bony and soft tissue structures surrounding the central spinal canal upon the underlying cauda equina. (Case courtesy of M. Rose)

Provocative or stress p/kMRI is an experimental technique currently under study that may be of major practical

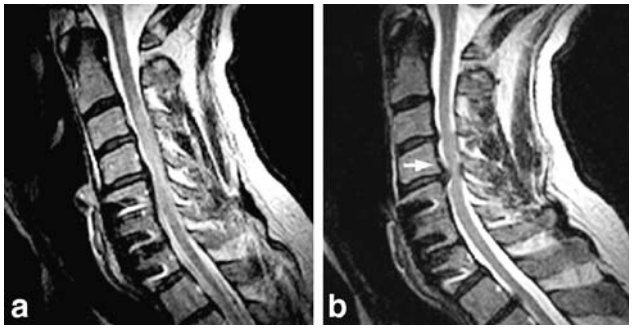

Fig. 10 Postoperative instrumented case of multilevel cervical spine fusion with disc herniation and spinal cord compression suprajacent to successfully fused levels; *adjacent level disease*. **a** Recumbent midline sagittal T2-weighted fast spin echo MRI (pMRI) shows an anterior fusion plate and vertebral body screws extending from C5 to C7. A minor posterior disc bulge is present at the C4–C5 level. **b** Upright-extension midline sagittal T2-weighted fast spin echo MRI (p/kMRI) shows minor posterior displacement of C4 on C5 indicating hypermobile intersegmental spinal instability above the level of the fusion. Note that the fused levels show no evidence of intersegmental motion, confirming successful surgical fusion stability. This image also importantly reveals further posterior protrusion/herniation of the intervertebral disc at the C4–C5 level and impingement upon the underlying spinal cord.

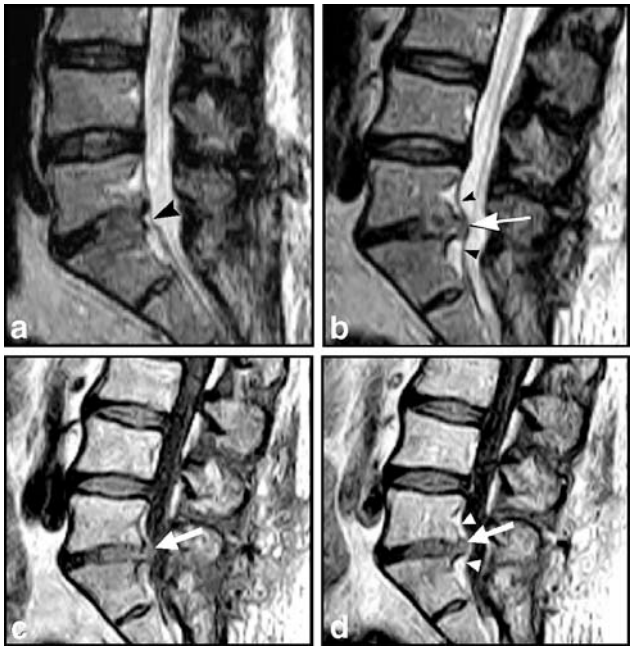

Fig. 11 Postoperative *recurrent fluid disc herniation* 8 months following partial right-sided discectomy in a patient with recurrent signs and symptoms. **a** Recumbent midline sagittal T2-weighted fast spin echo MRI (rMRI) shows a flat posterior surface (*arrow*) of the L5–S1 intervertebral disc. **b** Upright-neutral midline sagittal T2-weighted fast spin echo MRI (pMRI) reveals a focal posterior disc herniation extending from the L5–S1 intervertebral disc space. Note the tenting of the posterior longitudinal ligament and the thecal sac (*arrowheads*) secondary to the mass effect of the epidural disc herniation. **c** Upright-neutral midline sagittal T1-weighted fast spin echo MRI (pMRI) shows a poorly defined mass (*arrow*) extending posteriorly from the L5–S1 disc space. **d** Upright-neutral midline sagittal T1-weighted fast spin echo MRI (pMRI) following the intravenous administration of gadolinium demonstrates peripheral rim enhancement surrounding the centrally nonenhancing recurrent disc herniation (*arrow*). Also again note the tenting of the posterior longitudinal ligament and dura mater (*arrowheads*) secondary to the mass effect of the epidural disc herniation. (Case courtesy of M. Rose).

relevance in the future. By comparing images where the patient is pain- or symptom-free with images acquired in a specific position in which the patient experiences the pain or symptoms for which the examination is being performed, the imaging specialist may be able to clearly link the principal *abnormality* on the medical images with the relevant *clinical syndrome*. In this manner, provocative p/kMRI may become a truly *specific* diagnostic imaging method in cases of spinal disease and thereby ultimately improve patient outcomes.

With regard to *stress positional imaging* by pMRI, another unexpected application arose in practice. In a patient with weight-bearing upper sacral nerve root pain following a sports injury, a mobile posterior spinal facet process (zygapophysis) fracture was revealed that demonstrated increased lateral recess stenosis on the side and at the level of the monoradiculopathy (Fig. 12). This demonstration of

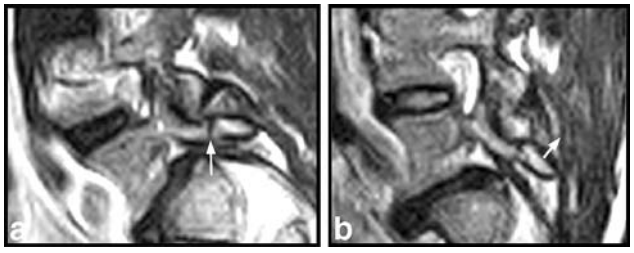

Fig. 12 *Mobile fracture* of posterior spinal facet process (zygapophysis). **a** Recumbent right parasagittal T1-weighted fast spin echo MRI (rMRI) reveals a linear hypointense area traversing the inferior articular process of L5, representing a facet process fracture. **b** Upright-neutral right parasagittal T1-weighted fast spin echo MRI (pMRI) shows posterior–superior displacement of the inferior articular process (*arrow*) indicating a mobile fracture fragment.

dynamic pathology that correlated with the clinical syndrome proved to be another example of both improved sensitivity and specificity. Yet another case in point was one of a work-related injury in a patient with ankylosing spondylitis who revealed an intersegmental fracture of a pathologically fused spinal level in the lumbar area (Fig. 13). This pathologic fracture showed motion (i.e., *pathologic hypermobility*) at this single, now unfused level on dynamic kMRI.

While some studies were not entirely free of motion artifacts, the upright images of the spine typically suffered

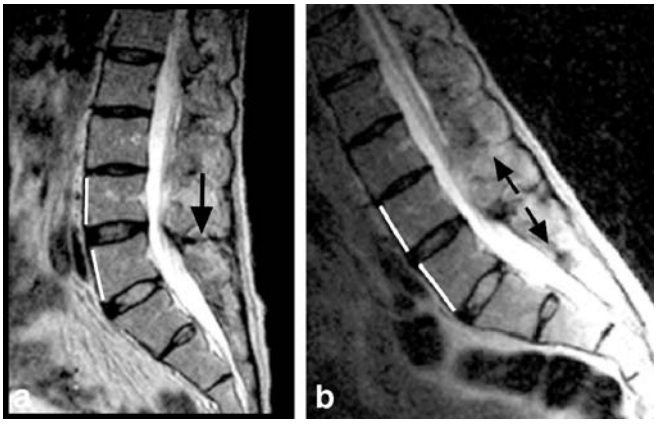

Fig. 13 Intersegmental fracture of pathologically fused spine associated with single-level *intersegmental hypermobility* in the case of ankylosing spondylitis. **a** Recumbent right parasagittal T1-weighted fast spin echo MRI (rMRI) reveals squaring of the anterior corners of all vertebrae and fusion of the spinous processes with the exception of L4–L5 consistent with ankylosing spondylitis. A linear hypointense area traverses a single interspinous space at L4–L5 (*arrow*), representing a fracture of a pathologically fused spine. Note the regular lordotic curvature of the lumbar spine as seen in the angled relationship of the anterior aspects of the L4 and L5 vertebral bodies (*lines*). Also observe the moderate stenosis of the central spinal canal at this level. **b** Upright-flexion midline sagittal T2-weighted spin echo MRI (p/kMRI) reveals splaying of the spinous processes at a single level, L4–L5 (*arrows*). Also noted is the loss of the lordotic curvature at L4–L5 as seen in the now parallel relationship of the anterior aspects of the L4 and L5 vertebrae (*lines*).

very little from such artifacts. At present, a *standing* sagittal sequence is felt to be necessary only for evaluating the lumbosacral spine in order to analyze true postural sagittal spinal curvature and for considering issues of *spinal balance*; importantly, an axial standing lumbosacral sequence should also be obtained to clearly determine the axial dimensions of the central spinal canal at these levels [71–74]. The remainder of the lumbosacral spine p/kMRI examination, and the entirety of the thoracic and cervical spine p/kMRI studies, may be performed in the *seated* position. In part, patient motion on the standing lumbosacral examination was overcome by simply placing the scan table at 5° posterior tilt, enabling the patient to "rest" against the table during the upright MRI acquisitions. Utilizing fast scan sequences (e.g., driven-equilibrium fast spin echo) for the upright-kinetic imaging portion of all spinal p/kMRI examinations also contributes to motion reduction (see later). Another useful application of the seat mounted on the scan table is in the patient with severe kyphosis due to senile osteoporosis or ankylosing spondylitis. In such cases, these patients often cannot lie down, making upright-seated imaging a valuable option.

The degree of chemical shift and magnetic susceptibility artifact was minor on all images, these types of artifact being directly related to field strength; such effects would be expected to be much less than half that experienced at 1.5 T. In addition, the degree of motion artifact from typical sources as the heart or CSF motion was typically minor, even without flow compensation overlay techniques; this source of artifacts is also loosely related to field strength, commonly being more severe for high-field MRI units.

Finally, in the patient with a possible critical stenosis of the spine in association with hypermobile instability or positional worsening of disc disease with consequent increased narrowing of the central spinal canal, long time period acquisition sequences are of concern in the patient who may have greater degrees of spinal cord or cauda equina compression during upright flexion–extension p/kMRI. For this purpose, very fast acquisition sequences have been implemented in order to screen for such critical abnormalities before going forward with longer time-period imaging studies (e.g., approximately 4–5 min). Driven-equilibrium fast spin echo acquisitions offer excellent quality imaging in a fraction of the time (e.g., approximately 17 s times two excitations equals 34 s) required of traditional sequences, and allow the rapid, safe imaging of almost any patient by p/kMRI. These fast high-resolution techniques may in the future be a major if not the sole method of imaging the spine using p/kMRI.

Conclusions

To conclude, the potential relative beneficial aspects of p/kMRI spinal imaging on this system over that of rMRI include clarification of true sagittal upright-neutral spinal curvature, revelation of occult degenerative spinal disease dependent on true axial loading (i.e., weight-bearing), unmasking of kinetic-dependent degenerative spinal disease (i.e., flexion–extension), and the potential ability to scan the patient in the position of clinically relevant signs and symptoms. Scanning the patient in the *operative position*, enabling the surgeon to have a true preoperative picture of the intraoperative pathologic morphology, is a topic currently under investigation [75]. This MRI unit also demonstrated low claustrophobic potential and yielded high-resolution images with little motion/chemical shift/magnetic susceptibility artifact. Overall, it was found that rMRI underestimated the *maximum degree* of degenerative spinal pathology and missed altogether its *dynamic* nature, factors that are ideally revealed with p/kMRI. Furthermore, p/kMRI enabled optimal linkage of the patient's clinical syndrome with the medical imaging abnormality responsible for the clinical presentation, thereby allowing for the first time an improvement in both imaging *sensitivity* and *specificity*.

On the basis of initial nonstatistical clinical experience with this unit, it is felt that mid-field MRI (i.e., 0.5–0.7 T) may prove to be the optimal field strength for routine, anatomic MRI of the spinal column in degenerative as well as other spinal disease categories [1, 2, 76–81]. In addition, the evidence thus far indicates that p/kMRI may prove to be efficacious to incorporate as a part of the clinical diagnosis–treatment paradigm in patients with spinal, radicular and referred pain syndromes originating from spinal pathology.

Acknowledgements The authors gratefully acknowledge the technical assistance of C.A. Green, J.F. Greenhalgh, M. Gianni, M. Gelbien, R.B. Wolf, and J. Damadian.

References

1. Jinkins JR, Dworkin JS, Green CA, Greenhalgh JF, Gianni M, Gelbein M, Wolf R, Damadian J, Damadian RV (2002) Upright, weight-bearing, dynamic–kinetic MRI of the spine: pMRI/kMRI. Riv Neuroradiol 15:333–356
2. Jinkins JR, Dworkin JS, Green CA, Greenhalgh JF, Gianni M, Gelbein M, Wolf R, Damadian J, Damadian RV (2003) Upright, weight-bearing, dynamic–kinetic magnetic resonance imaging of the spine—review of the first clinical results. J Hong Kong Coll Radiol 6:55–74
3. Smith TJ, Fernie GR (1991) Functional biomechanics of the spine. Spine 16:1197–1203
4. Smith TJ (1991) In vitro spinal biomechanics: experimental methods and apparatus. Spine 16:1204–1210

5. Marras WS, Granata KP (1995) A biomechanical assessment and model of axial twisting in the thoracolumbar spine. Spine 20:1440–1451
6. Resnick DK, Weller SJ, Benzel EC (1997) Biomechanics of the thoracolumbar spine. Neurosurg Clin N Am 8:455–469
7. Berne D, Goubier JN, Lemoine J et al (1999) The aging of the spine. Eur J Orthop Surg Traumatol 9:125–133
8. Boden SD, Wiesel SW (1990) Lumbosacral segmental motion in normal individuals: have we been measuring instability properly? Spine 15:571–576
9. Danielson BI, Willén J, Gaulitz A et al (1998) Axial loading of the spine during CT and MR in patients with suspected lumbar spinal stenosis. Acta Radiol 39:604–611
10. Frymoyer JW, Frymoyer WW, Wilder DG et al (1979) The Mechanical and kinematic analysis of the lumbar spine in normal living human subjects in vivo. J Biomech 12:165–172
11. Hedman TP, Fernie GR (1995) In vivo measurement of lumbar spinal creep in two seated postures using magnetic resonance imaging. Spine 20:178–183
12. Hilton RC, Ball J, Benn RT (1979) In-vitro mobility of the lumbar spine. Ann Rheum Dis 38:378–383
13. Inufusa A, An HS, Lim T-H et al (1996) Anatomic changes of the spinal canal and intervertebral foramen associated with flexion–extension movement. Spine 21:2412–2420
14. Mayoux-Benhamou MA, Revel M, Aaron C et al (1989) A morphometric study of the lumbar foramen: influence of flexion–extension movements and of isolated disc collapse. Surg Radiol Anat 11:97–102
15. Nachemson AL, Schultz AB, Berkson MH (1979) Mechanical properties of human lumbar spine motion segments: influences of age, sex, disc level, and degeneration. Spine 4:1–8
16. Nowicki BH, Haughton VM, Schmidt TA et al (1996) Occult lumbar lateral spinal stenosis in neural foramina subjected to physiologic loading. Am J Nueroradiol 17:1605–1614
17. Pennal GF, Conn GS, McDonald G et al (1972) Motion studies of the lumbar spine: a preliminary report. J Bone Jt Surg 54B:442–452
18. Penning L, Wilmink JT (1987) Posture-dependent bilateral compression of L4 or L5 nerve roots in facet hypertrophy: a dynamic CT-myelographic study. Spine 12:488–500
19. Schönström N, Lindahl S, Willén J et al (1989) Dynamic changes in the dimensions of the lumbar spinal canal: an experimental study in vitro. J Orthop Res 7:115–121
20. Sortland O, Magnes B, Hauge T (1977) Functional myelography with metrizamide in the diagnosis of lumbar spinal stenosis. Acta Radiol 355(Suppl):42–54
21. White AS, Panjabi MM (1978) The basic kinematics of the human spine: a review of past and current knowledge. Spine 3:12–29
22. Willén J, Danielson B, Gaulitz A et al (1997) Dynamic effects on the lumbar spinal canal: axially loaded CT-myelography and MRI in patients with sciatica and/or neurogenic claudication. Spine 22:2968–2976
23. Wilmink JT, Penning L, van den Burg W (1984) Role of stenosis of spinal canal in L4–L5 nerve root compression assessed by flexion–extension myelography. Neuroradiology 26:173–181
24. Friberg O (1987) Lumbar instability. A dynamic approach by traction–compression radiography. Spine 12:119–20
25. Fujiwara A, An HS, Lim TH et al (2001) Morphologic changes in the lumbar intervertebral foramen due to flexion–extension, lateral bending, and axial rotation: an in vitro anatomic and biomechanical study. Spine 26:876–882
26. Hayes MA, Howard TC, Gruel CR et al (1989) Roentgenographic evaluation of lumbar spine flexion–extension in asymptomatic individuals. Spine 14:327–331
27. Lee RR, Abraham RA, Quinn CB (2001) Dynamic physiologic changes in lumbar CSF volume quantitatively measured by three-dimensional fast spin-echo MRI. Spine 26:1172–1178
28. Panjabi MM, Takata K, Goel VK (1983) Kinematics of lumbar intervertebral foramen. Spine 8:348–357
29. Pearcy MJ, Tibrewal SB (1984) Axial rotation and lateral bending in the normal lumbar spine measured by three-dimensional radiography. Spine 9:582–587
30. Penning L, Wilmink JT (1981) Biomechanics of lumbosacral dural sac. A study of flexion–extension myelography. Spine 6:398–408
31. Revel M, Mayoux-Benhamou MA, Aaron C et al (1988) Morphological variations of the lumbar foramina. Rev Rhum Mal Osteo-artic 55:361–366
32. Stokes IA, Frymoyer JW (1987) Segmental motion and instability. Spine 12:688–691
33. Stokes IA, Wilder DG, Frymoyer JW et al (1981) Assessment of patients with low-back pain by biplanar radiographic measurement of intervertebral motion. Spine 6:233–240
34. Takayanagi K, Takahashi K, Yamagata M et al (2001) Using cineradiography for continuous dynamic-motion analysis of the lumbar spine. Spine 26:1858–1865
35. Wildermuth S, Zanetti M, Duewell S et al (1998) lumbar spine: quantitative and qualitative assessment of positional (upright flexion and extension) MR imaging and myelography. Radiology 207:391–398
36. Wisleder D, Smith MB, Mosher TJ et al (2001) Lumbar spine mechanical response to axial compression load in vivo. Spine 26:E403–E409
37. Wisleder D, Werner SL, Kraemer WJ et al (2001) A Method to study lumbar spine response to axial compression during magnetic resonance imaging. Spine 26:E416–E420
38. Zamani AA, Moriarty T, Hsu L et al (1998) Functional MRI of the lumbar spine in erect position in a superconducting open-configuration MR system: preliminary results. J Magn Reson Imaging 8:1329–1333
39. Leviseth G, Drerup B (1997) Spinal shrinkage during work in a sitting posture compared to work in a standing posture. Clin Biomech 12:409–418
40. Lowe RW, Hayes TD, Kaye J et al (1976) Standing roentgenograms in spondylolisthesis. Clin Orthop 117:80–84
41. Devor M, Rappaport ZH (1996) Relation of foraminal (lateral) stenosis to radicular pain. Am J Nueroradiol 17:1615–1617
42. Hasegawa T, An HS, Haughton VM et al (1995) Lumbar foraminal stenosis: critical heights of the intervertebral discs and foramina. J Bone Jt Surg 77-A:32–38

43. Pfirrmann CWA, Metzdorf A, Zanetti M (2001) Magnetic resonance classification of lumbar intervertebral disc degeneration. Spine 26:1873–1878
44. Shiwei Y, Haughton VM, Sether LA (1989) Criteria for classifying normal and degenerated lumbar intervertebral disks. Neuroradiology 170:523–526
45. Axelsson P, Johnson R, Strömqvist B (2000) Is there increased intervertebral mobility in isthmic adult spondylolisthesis? A matched comparative study using Roentgen stereophotogrammetry. Spine 25:1701–1703
46. Boden SD, Frymoyer JW (1997) Segmental instability: overview and classification. In: Frymoyer JW (ed) The adult spine: principles and practice. Lippincott-Raven, Philadelphia, pp 2137–2155
47. Dupuis PR, Yong-Hing K, Cassidy JD et al (1985) Radiologic diagnosis of degenerative lumbar spinal instability. Spine 10:262–276
48. Frymoyer JW, Selby DK (1985) Segmental instability: rationale for treatment. Spine 10:280–286
49. Fujiwara A, Lim T-H, An HS et al (2000) The effect of disc degeneration and facet joint osteoarthritis on the segmental flexibility of the lumbar spine. Spine 25:3036–3044
50. Pearcy M, Shepherd J (1985) Is there instability in spondylolisthesis? Spine 10:175–177
51. Ito M, Tadano S, Kaneda K (1993) A biomechanical definition of spinal segmental instability taking personal and disc level differences into account. Spine 18:2295–2304
52. Pope MH, Panjabi M (1985) Biomechanical definitions of spinal instability. Spine 10:255–256
53. Sato H, Kikuchi S (1993) The natural history of radiographic instability of the lumbar spine. Spine 18:2075–2079
54. Posner I, White AA, Edwards WT et al (1982) A biomechanical analysis of the clinical stability of the lumbar and lumbosacral spine. Spine 7:374–389
55. Wood KB, Popp CA, Transfeldt EE et al (1994) Radiographic evaluation of instability in spondylolisthesis. Spine 7:1697–1703
56. Yahia H, Drouin G, Maurais G et al (1989) Degeneration of the human lumbar spine ligaments. An ultrastructural study. Pathol Res Pract 184:369–375
57. Fujiwara A, Tamai K, An HS et al (2000) The interspinous ligament of the lumbar spine: magnetic resonance images and their clinical significance. Spine 25:358–363
58. Adams MA, Hutton WC, Stott JRR (1980) The resistance to flexion of the lumbar intervertebral joint. Spine 5:245–253
59. Dumas GA, Beaudoin L, Drouin G (1987) In situ mechanical behavior of posterior spinal ligaments in the lumbar region. An in vitro study. J Biomech 20:301–310
60. Hukins DWL, Kirby MC, Sikoryn TA et al (1990) Comparison of structure, mechanical properties, and functions of lumbar spinal ligaments. Spine 15:787–795
61. Panjabi MM (1992) The stabilizing system of the spine. Part 1. Function, dysfunction, adaptation, and enhancement. J Spinal Disord 5: 383–389
62. Panjabi MM, Goel VK, Takata K (1982) Physiologic strains in the lumbar spinal ligaments: an in vitro biomechanical study. Spine 7:192–203
63. Sharma M, Langrana NA, Rodriguez J (1995) Role of ligaments and facets in lumbar spinal stability. Spine 20:887–900
64. Fujiwara A, Lim TH, An HS (2000) The effect of disc degeneration and facet joint osteoarthritis on the segmental flexibility of the lumbar spine. Spine 25:3036–3044
65. Haughton VM, Schmidt TA, Keele K et al (2000) Flexibility of lumbar spinal motion segments correlated to type of tears in the annulus fibrosis. J Neurosurg 92:81–86
66. Thompson RE, Pearcy MJ, Downing KJW et al (2000) Disc lesions and the mechanics of the intervertebral joint complex. Spine 25:3026–3035
67. Twomey LT, Taylor JR (1983) Sagittal movements of the human lumbar vertebral column: a quantitative study of the role of the posterior vertebral elements. Arch Phys Med Rehabil 64:322–325
68. Cartolari R, Argento G, Cardello M et al (1999) Axial loaded computed tomography (AL-CT) and cine AL-CT. Riv Neuroradiol 12:33–44
69. Jinkins JR (1997) Posttherapeutic neurodiagnostic imaging. Lippincott-Raven, Philadelphia
70. Keller TS, Hansson TH, Holm SH et al (1989) In vivo creep behavior of the normal and degenerated porcine intervertebral disk: a preliminary report. J Spinal Disord 1:267–278
71. Jackson RP, Hales C (2000) Congruent spinopelvic alignment on standing lateral radiographs of adult volunteers. Spine 25:2808–2815
72. Lee C-S, Lee C-K, Kim Y-T et al (2001) Dynamic sagittal imbalance of the spine in degenerative flat back. Spine 26:2029–2035
73. Jackson RP, Kanemura T, Kawakami N et al (2000) Lumbopelvic lordosis and pelvic balance on repeated standing lateral radiographs of adult volunteers and untreated patients with constant low back pain. Spine 25:575–586
74. Jackson RP, Peterson MD, McManus AC et al (1998) Compensatory spinopelvic balance over the hip axis and better reliability in measuring lordosis to the pelvic radius on standing lateral radiographs of adult volunteers and patients. Spine 23:1750–1767
75. Stephens GC, Yoo JU, Wilbur G (1996) Comparison of lumbar sagittal alignment produced by different operative positions. Spine 21:1802–1807
76. Vitzthum H-E, Konig A, Seifert V (2000) Dynamic examination of the lumbar spine by suing vertical, open magnetic resonance imaging. J Neurosurg 93:58–64
77. Weishaupt D, Schmid MR, Zaneti M (2000) Positional MR imaging of the lumbar spine: does it demonstrated nerve root compromise not visible a conventional MR imaging? Radiology 215:247–253
78. Jinkins JR (2001) Acquired degenerative changes of the intervertebral segments at and suprajacent to the lumbosacral junction: a radioanatomic analysis of the nondiskal structures of the spinal column and perispinal soft tissues. Radiol Clin North Am 39: 73–99
79. Jinkins JR (2004) Acquired degenerative changes of the intervertebral segments at and supradjacent to the lumbosacral junction: a radioanatomic analysis of the nondiscal structures of the spinal column and perispinal soft tissues. Eur J Radiol 50:134–158
80. Jinkins JR (2002) Lumbosacral interspinous ligament rupture associated with acute intrinsic spinal muscle degeneration. Eur Radiol 12:2370–2376
81. Mitra D, Cassar-Pullicino VN, McCall IW (2004) Longitudinal study of vertebral type-1 changes of MR of the lumbar spine. Eur Radiol 14:1084–1432